Bridge Piers with Structural Fuses and Bi-Steel Columns. I: Experimental Testing

Samer El-Bahey[1] and Michel Bruneau, F.ASCE[2]

Abstract: Structural fuses, easily replaceable sacrificial elements to dissipate seismic energy while preventing damage to the gravity load-resisting structural system, are proposed as part of a multicolumn accelerated bridge construction (ABC) pier concept. Different types of structural fuses are investigated to compare the effect of each on ABC bridge bents. The piers of a three span-continuous bridge prototypes having two twin-column pier bents were designed using double-composite rectangular columns and structural fuses. Two corresponding 2/3-scale models were developed and were subjected to cyclic quasi-static tests. For the first specimen, steel-plate shear links (SPSLs) were installed between the columns as a series of structural fuses. Testing was performed, first up to a drift corresponding to the onset of columns yielding to investigate the effectiveness of adding the fuses in dissipating the seismic energy, then up to failure of the composite columns. The second tested specimen has buckling restrained braces (BRBs) as a series of structural fuses between the columns. The BRBs were then removed, and a cyclic test of the composite bent continued until failure of the columns. Both specimens exhibited stable hysteretic behavior, with the structural fuses also increasing stiffness and strength of the bent. Individual testing results for the SPSLs with various geometries and boundary conditions are then presented. **DOI: 10.1061/(ASCE)BE.1943-5592.0000234.**

CE Database subject headings: Buckling; Bracing; Steel columns; Seismic effects; Bridges; Piers.

Author keywords: Structural fuses; Buckling restrained braces; Steel plate shear links; Seismic; Bridges.

Introduction

Earthquakes can cause significant damage to bridge substructures. Providing reliable mechanisms for dissipation of the destructive earthquake energy is key, both for safety and to limit the forces in structural members. The concept of designing sacrificial members to dissipate the seismic energy, while preserving the integrity of other main components, is known as the structural fuse concept. The term structural fuse can be found in the literature at least going back to Roeder and Popov (1977) as part of their proposed eccentrically braced frame concept for steel frames and in much subsequent research (e.g., Fintel and Ghosh (1981) used a similar capacity design concept and designated plastic hinging of the beams to be structural fuses), although in much past research, the fuses were not easily replaceable. Wada et al. (1992) expanded on the structural fuse concept by defining damage-controlled or damage tolerant structures in which the structure was considered as two separate components, namely, a moment frame designed to resist 80% of the lateral loads and, second, special bracing as passive energy dissipation elements dedicated to provide energy dissipation under the loads resulting from strong ground motions. Conner et al. (1997) demonstrated that the effectiveness of the damage-controlled structures concept depends on the energy dissipation capacity of the bracing devices used and the ability of the primary structure to remain elastic during a major seismic event, which is more easily achieved when high strength materials, for the primary structure are combined with low strength ones for the bracing system. Further developments were proposed by Shimizu et al. (1998), Wada and Huang (1999), and Huang et al. (2002). Wada and Huang (1995) implemented an approach on the basis of the balance of energy to design tall building structures having either hysteretic dampers or viscous dampers. A comprehensive study of damage-controlled structures in Japan was presented by Wada et al. (2000). That paper presented some research work done on the development of the damage-controlled structures concept and its potential to design new constructions and to retrofit existing structures. A dynamic analysis method was proposed for three-dimensional frames with elements used to develop the structural fuse concept. Building on that prior work, Vargas and Bruneau (2009a, b) provided a systematic design procedure to achieve a structural fuse concept to limit damage to disposable structural elements for any general structure, without the need for complex analyses.

All the previous work on the structural fuse concept focused on implementations in buildings. While inelastic deformations have been relied upon to achieve ductile performance for bridges, implementation of the structural fuse concept has not been implemented in standard bridge's piers [although replaceable fuses have been implemented between the towers of one signature bridge (Goodyear and Sun 2003], and it can be argued that ductile diaphragm concepts (Bruneau et al. 2002) embody the same principles. One such structural fuse concept for a bridge pier, which could be of benefit for both new and existing bridges, is considered here. Here, fuses are added to a two-column bridge bent to increase its strength and stiffness, while dissipating the seismic energy through hysteretic behavior and while keeping the bridge columns elastic. The bridge bent in this particular application consists of segmental composite columns built in stacked segments but continuous after concrete curing. Several types of structural fuses can be used in bridges; the focus here is on two specific types,

[1]Structural Engineer, Stevenson & Associates, Phoenix, AZ (corresponding author). E-mail: selbahey@gmail.com

[2]Professor, Dept. of Civil, Structural, and Environmental Engineering, State University of New York, Buffalo, NY.

Note. This manuscript was submitted on August 12, 2010; approved on February 22, 2011; published online on February 24, 2011. Discussion period open until June 1, 2012; separate discussions must be submitted for individual papers. This paper is part of the ***Journal of Bridge Engineering***, Vol. 17, No. 1, January 1, 2012. ©ASCE, ISSN 1084-0702/2012/1-25–35/$25.00.

namely steel plate shear links (SPSLs) and buckling restrained braces (BRBs).

First, BRBs are used here as structural fuses. Typical BRBs consists of a steel core encased in a steel tube filled with concrete. The steel core carries the axial load while the outer tube, via the concrete, provides lateral support to the core and prevents global buckling. Typically a thin layer of material along the steel core/concrete interface eliminates shear transfer during the elongation and contraction of the steel core and also accommodates its lateral expansion when in compression (other strategies also exist to achieve the same effect). This gives the steel core the ability to contract and elongate freely within the confining steel/concrete-tube assembly. A variety of these braces having various materials and geometries have been proposed and studied extensively since the mid-1990s (Clark et al. 2000; Black et al. 2002; Hasegawa et al. 1999; Iwata et al. 2000; Lopez et al. 2002; López and Sabelli 2004; Mamoru Iwata 2006; Sabelli et al. 2003; Saeki et al. 1995). A summary of much of the early development of BRBs which use a steel core inside a concrete-filled steel tube is provided in Fujimoto et al. (1988). Since the 1995 Kobe earthquake, BRBs have been used in numerous major structures in Japan (Reina and Normile 1997). The first tests in the United States were conducted in 1999 (Aiken et al. 2002), followed by multiple implementations.

Here, because of the short distance between columns, a new type of BRB was used (Jason Powell, Star Seismic, personal communication, 2010). Its specific design eliminates the transition length between the yielding core and the nonyielding part found in conventional BRBs, which allows for shorter BRBs. It is also entirely made of steel (i.e., without a concrete fill) which reduces its weight substantially.

The BRB assembly used and shown in Fig. 1 consists of a yielding circular steel core, welded to four oversized gusset plates (two at each end). The steel core is inserted in an outer hollow steel tube, which is used to prevent the local buckling of the yielding core when in compression. The outer hollow steel tube is stiffened by circular steel plates at equal distances along its length for this purpose. This assembly is inserted in a bigger hollow steel circular tube; this outer tube is kept in place by tack welds to the inner stiffeners. The yielding core is welded to the gussets, themselves connected to the main structure by pins. The inside of a BRB is not visible once assembled and delivered to the site; for that reason, quality control mechanisms are primordial. More details on the assembly of the BRB is presented in El-Bahey and Bruneau (2010).

The second type of fuse element considered here is a steel-plate shear link (SPSL), shown in Fig. 2. The initial proposed concept consisted of an hourglass-shaped steel plate designed to yield in shear at $0.6\sigma_y$ and restrained from out-of-plane buckling by an unbonded encasement. Because of some unexpected weld failures presented later, the unbounded material was removed, and testing continued with links unrestrained from lateral bucking. Individual SPSLs were then tested with different geometries and lateral support conditions. The initial concept development and the analytical results of the individual SPSL tests are presented in a companion paper (El-Bahey and Bruneau 2011)

Prototype Bridge and Specimen

The prototype bridge considered is a continuous bridge having three equal spans of 36 m, and two 9-m high twin-column

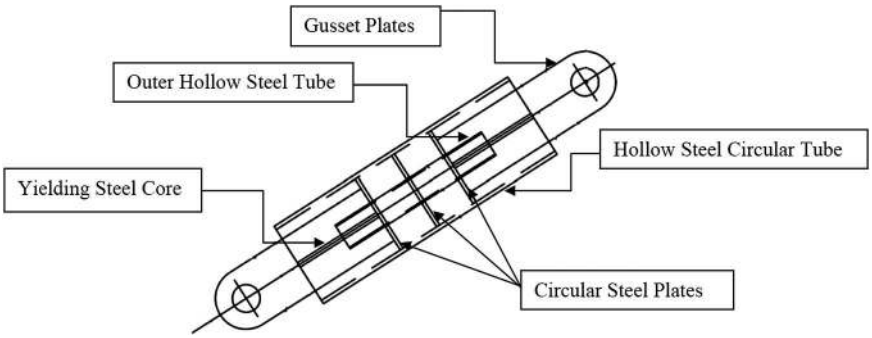

Fig. 1. BRB assembly

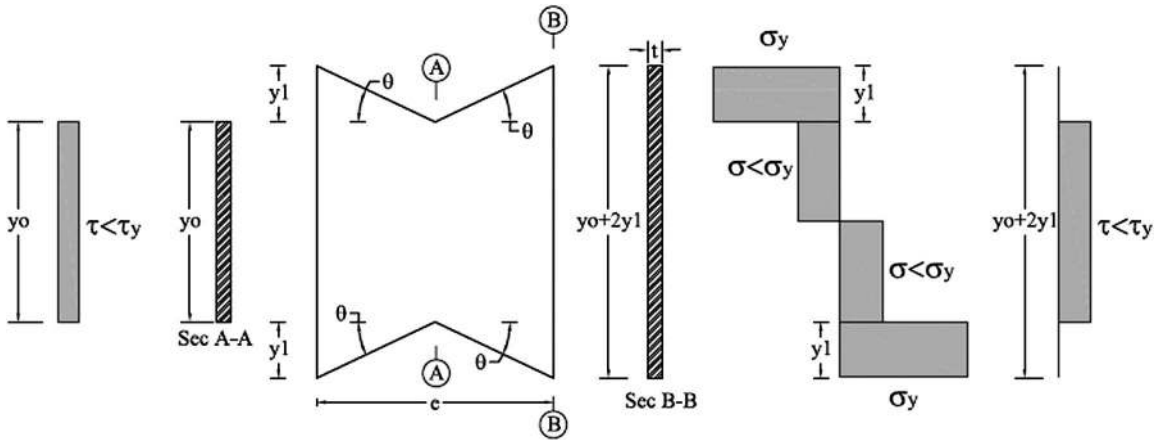

Fig. 2. Assumed stress distribution in mid- and endplates

pier bents. The gravity load design (dead and live loads) has been done according to the AASHTO LRFD (2009) specifications, and the columns were designed as composite rectangular columns. These composite columns used here to achieve the accelerated bridge construction (ABC) objectives were made of bi-steel, which is a system of double-skin steel-concrete-steel high-performance rapid erect panels (Bowerman et al. 1999). These panels are composed of steel plates connected by an array of transverse friction-welded shear connectors and filled with concrete. That system is suited to extensive prefabrication (e.g., penetrations, attachments, connections, and coatings) prior to site delivery. The composite columns were used here to investigate their ductility and to demonstrate a possible mean to simultaneously meet accelerated construction objectives. End plates were welded to create a box section, which then served as formwork for the concrete.

A 2/3-scale specimen was chosen because of limitations of the Structural Engineering and Earthquake Simulation Laboratory (SEESL) at the University at Buffalo. In a first specimen (labeled S1), SPSLs were installed between the columns to serve as a series of structural fuses. A second specimen used BRBs as the series of structural fuses between the columns (labeled S2-1). For that specimen, as subsequently described, the BRBs were removed to test the composite bent alone (labeled specimen S2-2). The links in each specimen (S1 and S2-1) were designed to develop their theoretical plastic strength at a maximum horizontal force of 1,250 kN. To accommodate large possible specimen overstrength, 2 of 1,777 kN actuators were used. The resulting design made use of a link with thickness equal to 5 mm. An 8 mm gusset plate was also welded to the columns of the first specimen over their entire height to which the SPSLs could be connected. The gusset plate and its welds were also designed to remain elastic during the testing procedure. The cross section of specimen S1 is shown in Fig. 3.

Bolted connections were used for the specimens' fuses, assuming that they would likely be preferred in practice to facilitate fuse replacement (an important objective). Many combinations of strength and stiffness are possible for structural fuses systems. Results from analytical parametric studies (El-Bahey and Bruneau 2010) suggest best performance for larger increases in stiffness coupled with more fuse ductility before column yielding.

For the second specimen (with BRBs as structural fuses between the columns), six BRBs having specified yield strength of 533 kN and $\sigma_y = 355$ MPa, and a core length of 300 mm and total BRB length of 600 mm were also designed to meet the structural fuse concept described previously. A typical BRB is shown in Fig. 4. Pin-ended connections were used to eliminate moment and shear at the connection points and to allow rotation of the BRBs during specimen sway.

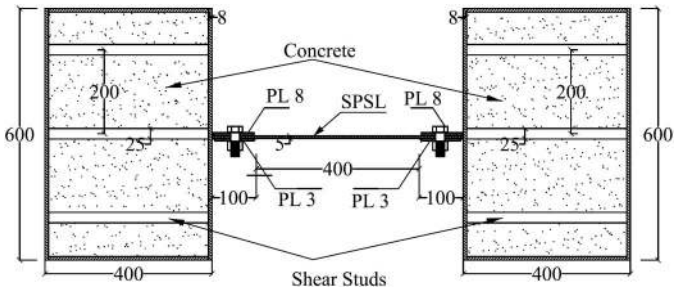

Fig. 3. Column cross-section details and dimensions in mm for Specimen S1 (plan view cross section)

Fig. 4. BRB used in specimen (S2-1)

Experimental Setup, Instrumentation, and Loading Protocol

Segmental columns filled with concrete were used for the purpose of this experimental study; each column consisted of four bi-steel segments fabricated with different heights, and all having the same cross-sectional dimension. While it would have been possible to have the columns constructed as continuous over their entire height, the segmental approach was deliberate to illustrate the construction procedure that could be followed on-site in the perspective of accelerated bridge construction for taller piers. As such, the columns were stacked over one another and welded with full penetration welds.

The cross section consisted of a 600 mm × 400 mm bi-steel panel, with steel plate thickness equal to 8 mm, with 25 mm diameter shear connector bars spaced at 200 mm c/c in both directions. The lower-column segment was set to be 815 mm tall, allowing 600 mm to be embedded in the foundation base (FB), and 215 mm above the FB to be connected to the above segment. The following two middle segments were 2,600 mm tall, while the upper-column segment height was 1,600 mm.The cap beam (CP) consisted of three parts, all the same height of 1,250 mm, with different widths. The cap beam was designed to be relatively rigid compared to the column segments and also to resist M_p and V_p of the columns, while remaining elastic.

Because two Material Testing Systems (MTS) servocontrolled static-rated actuators were used to apply lateral loads to the specimens, a loading beam (LB) was necessary to transfer the load from the two actuators to the specimen. The LB was also designed to remain elastic. The FB was also designed to remain elastic for the maximum actuator load that could be applied to the specimen with a factor of safety of 1.5.

The global response of the structure in displacements was obtained from string-pots installed at different levels from the base to the top of the frame. Optical coordinate tracking probes (Krypton sensors) were also distributed on the columns up to their mid heights (because of camera range constraints) to measure displacement response at specific points. The seismic response of the columns was obtained from strain gages installed at critical points (top and bottom of each column), to determine whether these columns remain elastic during the test. Axial deformations of the BRBs were measured with string-pots installed in parallel with the braces and connected to the gusset plates. To verify if slippage or uplift

occurred at the specimen base, horizontal and vertical transducers were installed at its four corners.

The loading of all specimens was originally intended to proceed following quasi-static displacement control cycles carried out in accordance with the Applied Technology Council ATC 24 loading protocol [Applied Technology Council (ATC) 1992], adjusted during the tests as necessary in response to specific observed behaviors. For the tests of specimens with structural fuses in place, (i.e., specimens S1 and S2-1), it was decided to stop testing before yielding occurred in the columns to be able to test the undamaged columns on their own in following tests. For this purpose, it was necessary to estimate the value of the horizontal displacements at the top of the specimen that would correspond to the onset of yielding of both the structural fuse elements and the columns. Preliminary push-over analyses using ABAQUS models were conducted prior to testing to estimate these values. Since actual material properties were unavailable at that time, the typical material properties of A572 grade 50 steel and the specified concrete strength of 28 MPa were used in the analysis. Analytical predictions failed for two reasons: (1) Because of the unanticipated flexibility of the reacting strong wall, the ABAQUS model predicted a stiffer system and thus smaller values of yield displacements for both the fuses and the bare frame; (2) The actual material yield strength of the frame turned out to be approximately 40% more than the typical A572 Gr. 50 steel material assumed in the preliminary finite element analysis which thus predicted yield displacements less than actual. A decision was made during testing to experimentally define the yield values and proceed by recalibrating the displacement protocol from that value. As a result, an extensive number of elastic cycles were performed before reaching the experimentally defined yield values, from which all the other loading values were recalibrated. Furthermore, three tests were done on specimen S1 because of unexpected weld failures as will be described in the next section, which resulted in applying more elastic cycles than originally anticipated.

In all cases, testing of all specimens was controlled by observing the real-time plotting of the hysteretic curves of the applied load versus top lateral displacement for specimens S1, S2-1, and S2-2 and adjusting the applied displacements to achieve the target load protocol. Also, the average strain at the bottom of the columns was monitored after each cycle to experimentally identify the yield displacement of the frame, Furthermore, cameras were installed at the bottom of the columns and close to the fuses to identify signs of local buckling.

Experimental Results and Observations

Hysteretic plots of specimen base shear versus top displacement are shown in Fig. 5 for specimens S1, S2-1, and S2-2. Fig. 6 shows specimens S1, S2-1, and S2-2 prior to testing.

Specimen (S1)

Testing of specimen S1 proceeded in three steps because of unexpected failures in the full penetration welded splices connecting the columns' segments. In the first part of the test, the specimen remained elastic up to a displacement equal to 25 mm (0.36% drift). At 50 mm displacement (0.72% drift), the lateral load resisted by the specimen dropped by 80% from 613 kN to 129 kN. This was because of an unexpected weld failure in the column segment connection in the lower end of the east column.

An investigation was conducted to understand the cause of the failure, and a decision was made to repair/reinforce both lower splices of the specimen (the fractured and unfractured ones) by adding a 16 mm thick, 50 mm wide steel plate to create a new fillet-welded splice all around the columns on top of the existing splice locations. These new splices were generously overdesigned to preclude any further failures at those locations. Reasons for these brittle failures are briefly explained later.

Also, a decision was made to take out the buckling restraints attached to the SPSLs, because at that time, the cause for the incorrectly predicted fuse yielding could not be explained; the intent was to make sure that the fuses would yield before the columns, and since deformation of the fuses was not visible because of the presence of the restraints, it was judged prudent to remove them for the next phase of testing. Taking out the restraints decreases the contribution of the links to the total strength of the system because they will buckle and behave more like a steel-plate shear wall with perforations as explained in the companion paper (El-Bahey and Bruneau 2011). The ability to develop structural fuses nonetheless remained.

Since the specimen was almost completely elastic at the time of the weld failure, the testing protocol was restarted from the beginning. Removing the restraints did not affect the elastic stiffness of the total system; this is because of the fact that the unrestrained SPSLs behave similarly to the restrained SPSLs in the elastic range, and differences start to occur only after the unrestrained SPSLs start to buckle (El-Bahey and Bruneau 2011). All the previously applied cycles were reapplied with similarly observed elastic behavior (but without weld fracture this time). Testing continued with applied lateral displacements beyond the one at which the connection splice failure had previously occurred. At 37.5 mm displacement (0.54% drift), signs of yielding started to occur on the middle links. The yield point of the fuses was experimentally defined as the onset of softening that occurred on the hysteretic curve. Yielding had propagated to all links when 100 mm displacement (1.5% drift) was reached. At 100 mm displacement (1.5% drift), the lateral load resisted by the specimen dropped by 41% from 887 kN to 507 kN. This was because of another unexpected weld fracture in the column splice in the upper end of the west column.

To better understand the cause of the recurring undesirable weld performance, a more intensive investigation was conducted on the type of welding material used and the actual yield strength of the steel used for the bi-steel panels. It was discovered that the yielding and fracture stress were approximately 40% more than expected, with yield strengths of 470 MPa, and 520 MPa, and ultimate strengths of 530 MPa and 580 MPa, respectively. Matching electrodes were E70. A few weld defects (incomplete beveling and minor undercuts) also detrimentally affected behavior of these full penetration welds).

The same repair/reinforcement detail as done previously for the lower splices was implemented for both the upper splices of the specimen (the fractured and unfractured ones) to create a new fillet-welded splice all around the columns on top of the existing splice locations.

Testing restarted by repeating the cycles at a displacement of 75 mm (1.1% drift). At 112.5 mm displacement (1.6% drift), minor signs of yielding of the lower-west column were observed. At that drift, it was determined that the part of the experiment intended to illustrate the structural fuse concept had been completed because a further increase in displacement would have resulted in the columns yielding. Fig. 7 shows the links at this stage of the test.

Nevertheless, testing continued for the specific purpose of observing the ultimate behavior of the bi-steel columns in this particular application. Local buckling at the west side of the lower-west column started to appear at 150 mm displacement (2.2% drift) as shown in Fig. 8(a), while fracture started to occur at the same drift level at the east side of the column and propagated rapidly.

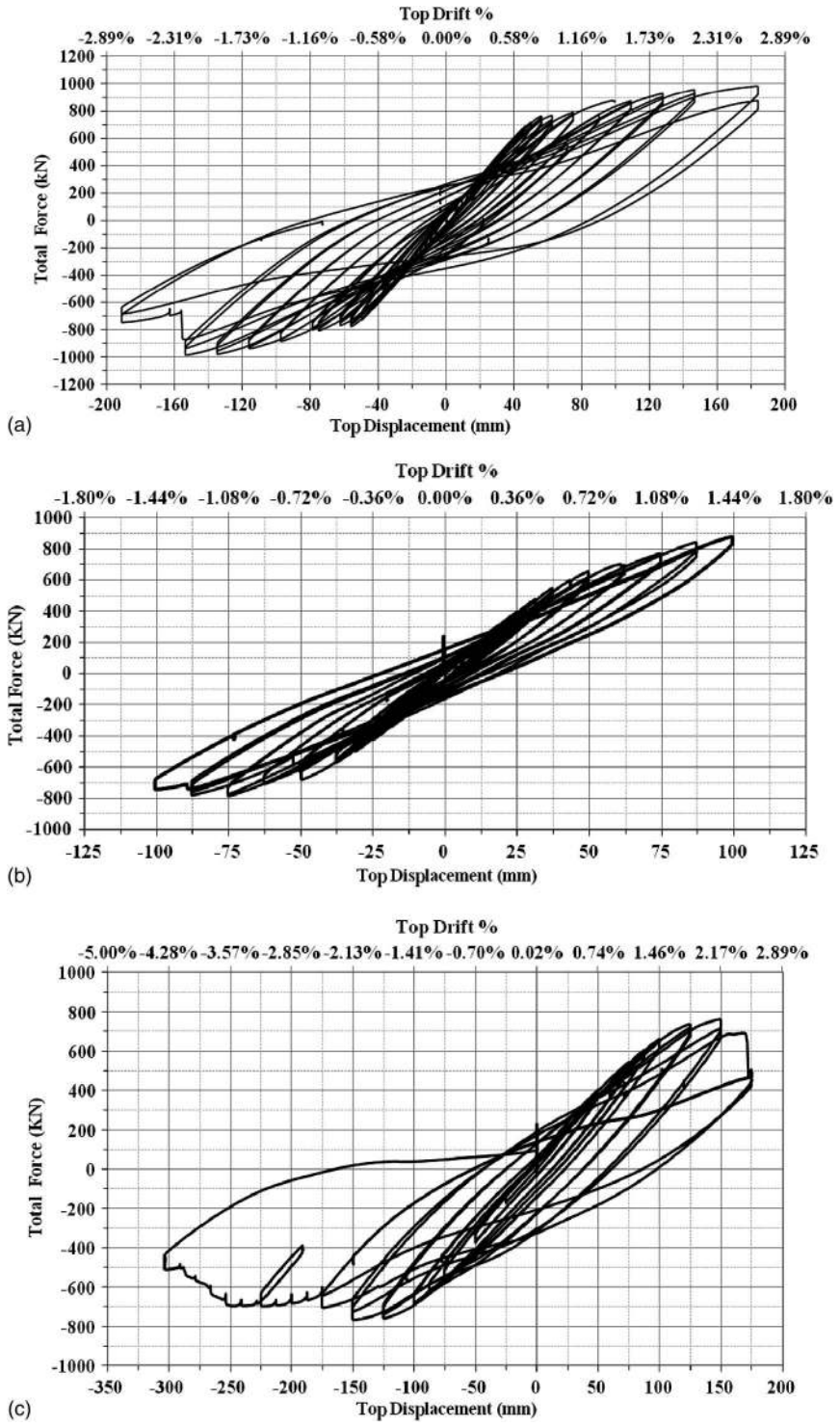

Fig. 5. Specimen hysteresis: (a) S1; (b) S2-1; (c) S2-2

The column was completely fractured along its west side as shown in Fig. 8(b) at 187.5 mm displacement (2.7% drift), and the load dropped from 700 kN to 420 kN at that point.

The lower-east column started to locally buckle at 187.5 mm displacement (2.7% drift). At that point, the west column was severely damaged, and, as far as observing further damage to that column, imposing further cycles of inelastic displacement to that column from that point onward was judged to be of no benefit. However, it was decided to continue testing monotonically, imposing compression on the west column and tension on the east column until the east column was completely damaged. Testing continued until a displacement of 225 mm (3.3% drift). At that point, crushed concrete started to come out of the fractured ends of the extensively damaged west column. Excessive buckling was observed on the east column at that stage, accompanied by a minor fracture that started to occur. It is shown in the pictures that the buckled shape is affected by the presence of the bi-steel shear connector, which appeared to be effective as a buckling restraint point. Unfortunately, the test ended when another unexpected sudden splice failure occurred, this time in the midheight splice of the west column at

Fig. 6. Specimens prior to testing: (a) S1; (b) S2-1; (c) S2-2

Fig. 7. SPSL's yielding at 1.6% drift

225 mm displacement (3.3% drift) to end that test. While some weld failure occurred during testing, it is believed that these failures where for that particular case. With due quality control of the welds and steel properties, it is believed that these ABC systems are effective, time saving, and economical.

Specimen (S2-1)

To avoid a repeat of the problems because of weld failures, all splices of specimen S2-1 were reinforced prior to the test by adding steel plates at the locations of all the welded splices between the column segments (plates and weld sizes identical to those in the prior specimen).

Testing started following the same loading protocol. Specimen S2-1 reached a displacement of 37.5 mm (0.54% drift) and exhibited completely linear behavior. At 50 mm displacement (0.72% drift), signs of yielding were observed by softening of the hysteretic loop; this was attributed to the yielding of the BRBs, because no sign of yielding was observed in any of the columns. No strain gages could be installed on the BRBs, so this yielding could only be inferred from the shape of the hysteretic loops.

Up to 87.5 mm displacement (1.3% drift), no evidence of yielding or buckling was observed in the column bases. At 100 mm displacement (1.45% drift), the first signs of minor local buckling were observed in the bottom-east column. At this point, testing was terminated to preserve the integrity of the columns for a final test in which only the bare frame was to be tested (without any fuses between the columns) and was needed for comparison purposes. Fig. 9 shows the hysteretic behavior for one of the BRBs installed (third from top) plotted against the total system force. The yielding of this particular BRB occurred at approximately 0.6 mm axial displacement, and an elongation of approximately 6 mm was

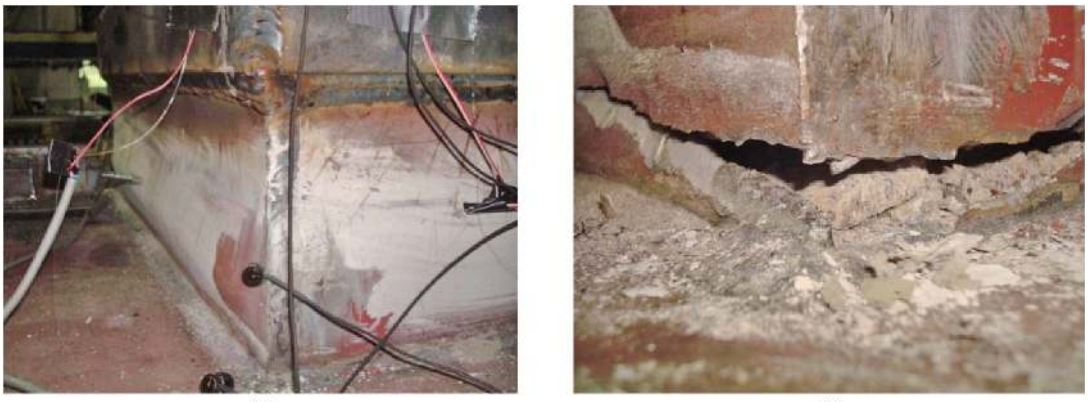

Fig. 8. (a) Local buckling of west column 2.2% drift; (b) fracture at 2.7% drift

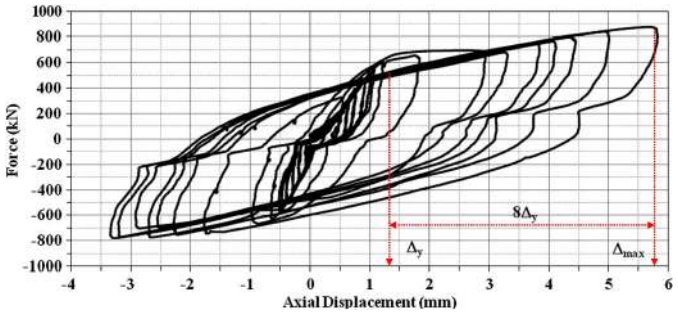

Fig. 9. Hysteretic behavior for BRB (third from top)

observed, from which an approximate ductility value of 8 is observed. The other BRBs exhibited different ductility values ranging from 3 to 17 depending on their location along the height of the columns (El-Bahey and Bruneau 2010). A small amount of slippage occurred because of the pin connection of the BRBs.

Specimen (S2-2)

To quantify the contribution of the fuses to the strength and stiffness of the total system, bare frame testing was essential. After terminating testing on specimen S2-1, the BRBs were removed.

A second objective of this test was to investigate the cyclic behavior of the bi-steel columns. Toward this end, the bare frame was subjected to cycles of progressively increasing lateral displacement magnitudes until failure of the columns occurred. Linear behavior was observed, as confirmed by the hysteretic curve shown in Fig. 5(c) and also by the average strains read from the gages at the bottom of the columns up to 100 mm displacement (1.45% drift) where signs of local buckling were observed at the east side of the bottom-east column. At 100 mm displacement (1.45% drift), buckling propagated to the north side of the bottom-east column.

At 125 mm displacement (1.81% drift), a minor crack of approximately 12.5 mm was observed in the northeast and southeast corners, weld of the bottom-east column. Because of the concern that this might be an isolated weld defect that could lead to unrepresentative response, a decision was made to fix the welds before testing continued. Fixing the welds was done by adding three weld passes of approximately 125 mm on top of the existing weld at the specific fracture location. At 150 mm displacement (2.17% drift), local buckling started to develop on the west side of the bottom-west column. A minor crack on the same face of the column was observed at the connection between the plate and the internal shear connectors. Another crack reappeared on top of the weld reinforcement at 150 mm displacement (2.17% drift). At 150 mm displacement (2.17% drift), a similar crack was observed on the east side of the bottom-east column. At the same time, a huge crack at the southeast corner of the east column was observed, and concrete started spalling out of the column.

Testing continued to 175 mm displacement (2.5% drift), at which the lateral load resisted by the specimen dropped 44% from 711 kN to 400 kN. As testing continued, to better understand the progression of the failure mechanism (and because the specimen had a nonnegligible residual strength), the crack propagated across the south side of the east column, and the east column was totally damaged at this stage.

It was not deemed beneficial to cycle further beyond that point, but the west column was still intact, having suffered only from local buckling. So it was decided to apply one more half cycle up to a displacement that would make the west column totally fails. The fractured column would be in compression during that half cycle, making that last stage of testing possible. At 175 mm displacement (2.5% drift), a minor crack started to appear at the northwest corner of the bottom-west column. The crack started to grow and propagate as displacement was increased in the same direction. At the same time, the east column was suffering major damage at 200 mm displacement (2.9% drift). At 225 mm displacement (3.26% drift), the crack at the northwest corner of the west column propagated, and concrete started spalling from the southeast corner of the east column. At 250 mm displacement (3.62% drift), the applied load started to drop gradually as shown on the hysteretic curve, and the existing crack on the west face of the west column further propagated. At the same time, another large crack developed at the northeast corner of the bottom-east column, and concrete rubble started to escape from the crack opening as shown in Fig. 10(a). At 300 mm displacement (4.35% drift), the west column had developed 600 mm long cracking along its base and had extensive local buckling, and concrete rubble started escaping from the northwest corner crack as shown in Fig. 10(b). Testing was then terminated at that stage.

Comparison of Results

Average strains for column sides at the onset of column yielding (1.6% drift) are shown in Fig. 11. Specimens S1 and S2-1 respectively, showed that no significant yielding has occurred in the columns, and the hysteretic behavior is due to the fuses yielding. A comparison for the values of the elastic stiffness, base shear, ductility, drift, and strength reduction for each specimen is shown in

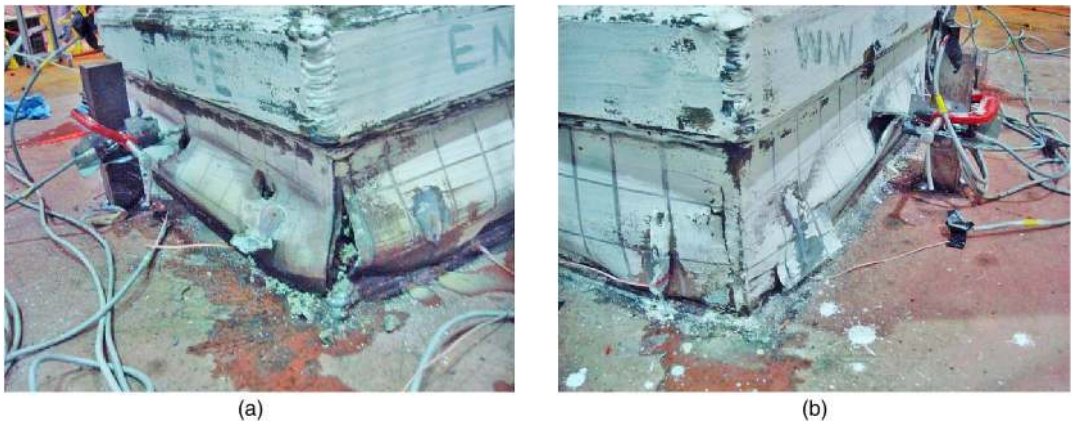

Fig. 10. (a) Damage at east column at 3.62% drift; (b) damage at west column at 4.35% drift

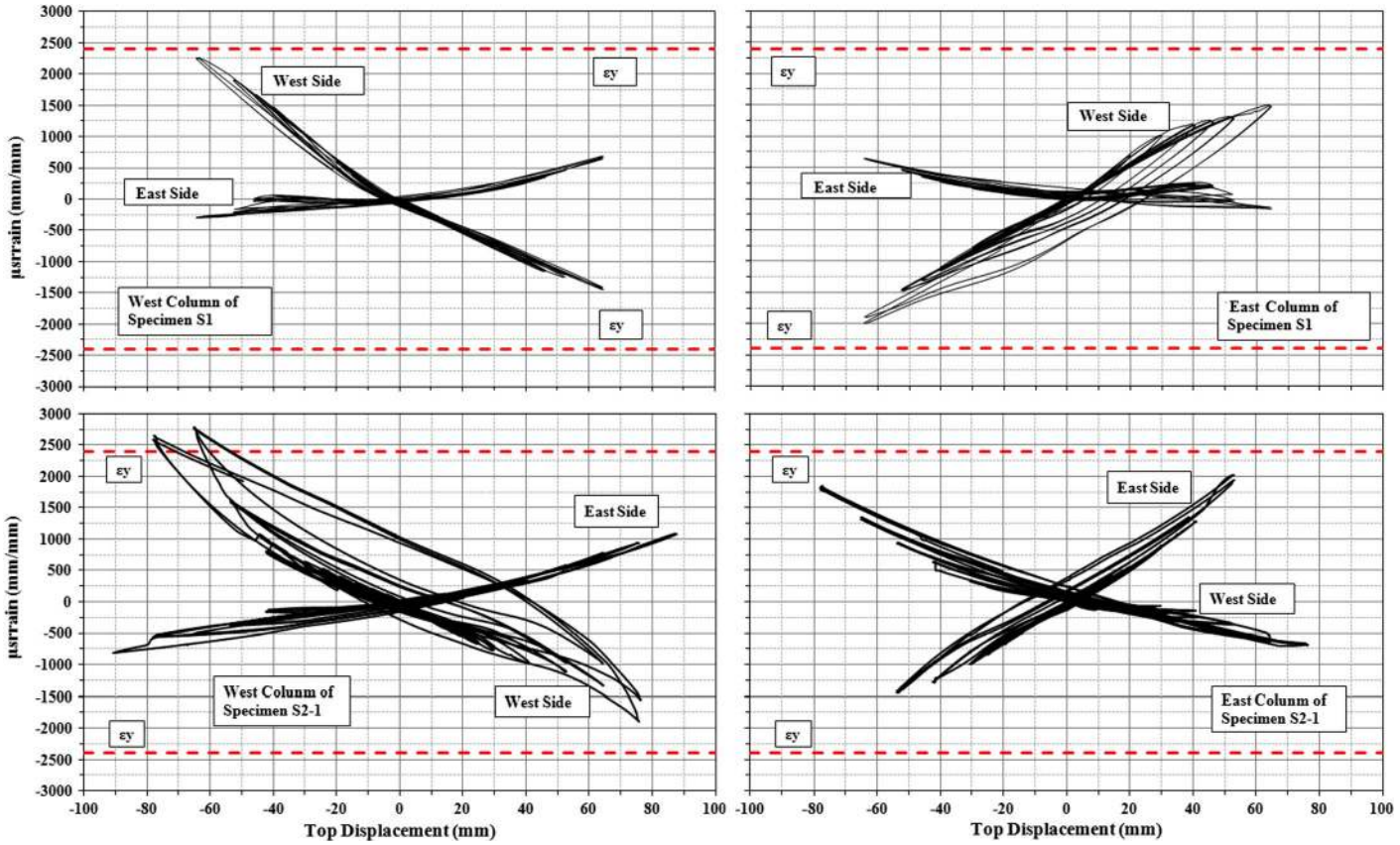

Fig. 11. Average strains of column sides for Specimens S1 and S2-1

Table 1. Specimen S1 performed successfully after unexpected failures and repairs of the welded splices between the segmental columns. After fixing the welds, the specimen behaved in a stable ductile manner until it reached 225 mm displacement (3.3% drift). The onset of column yielding was observed at 100 mm displacement (1.6% drift) accompanied with minor local buckling at the bottom of one column. A base shear of 875 kN was observed at that level of drift. Failure of the specimen was due to a fracture at the bottom of both columns because of low cycle fatigue, which developed at the locations of repeated local buckling. A strength reduction of 33% from the peak value was observed at the maximum drift reached when testing had to stop because of the failure of a midheight column splice (this failure could not be repaired). Adding the SPSLs increased the elastic stiffness of the bare frame by 80%, while the strength increased by 31%. This strength increase was less than originally expected from the SPSLs because of the removal of the buckling restraints, which decreased the SPSLs strength by 30%.

Specimen S2-1 was also successfully tested up to a drift corresponding to the onset of column yielding at 100 mm displacement (1.6% drift); a base shear of 881 kN was observed at that level of drift. As indicated previously, because it was essential to keep the integrity of the column for testing the bare frame alone, testing stopped after minor signs of local buckling were observed on one of the columns. No failure was expected from this specimen, but yielding of the BRBs dissipating the seismic energy was observed on the overall hysteretic behavior of the specimen. Adding the BRBs increased the elastic stiffness of the bare frame by 80%, while the strength increased by 20%.

Specimen S2-2 was tested successfully to 175 mm displacement (2.5% drift) until the east column failed. Noncyclic testing continued in the other direction up to a displacement of 300 mm (4.45% drift) to fail the other column. Fracture occurred at the bottom of both columns because of low cycle fatigue, which developed at the locations of repeated local buckling. It is shown in Table 1 that all specimens did not reach the setup design strength of 1,250 kN; this is because this strength was designed taking into account the presence of out-of-plane restraints for the SPSLs (which were removed at a previous testing stage).

Table 1. Summary of Peak Results

Specimen	Elastic stiffness (kN/mm)	Base shear at column yielding (kN)	Maximum base shear (kN)	Fuse ductility at column yielding	Fuse ductility at maximum drift	Column yielding drift (%)	Maximum drift (%)	Strength reduction at maximum drift (%)
S1	19	875	982	4	8	1.6	3.3	33
S2-1	21.5	881	—	4	—	1.6	—	—
S2-2	8	666	806	—	—	1.6	4.3	29

Fig. 12. Pentograph system

Experimental Testing of Individual Fuses

Several SPSLs having the same dimensions as the ones used in the bridge pier test were selected for individual quasi-static testing. Some having lateral restraints using a fiberglass building panel material, and some are without lateral restraints to compare their behavior with the restrained ones and evaluate the amount of strength lost by the fuses after removing the restraints.

The test setup shown in Fig. 12 was originally designed by Berman and Bruneau (2005). The setup is a pantograph that was designed to apply a shear force on short-length specimens. The pantograph functions to prevent the rotation of the loading beam while allowing the link to deform unrestrained in the axial and horizontal directions, preventing the introduction of axial load in the link when deformed in shear and flexure. The loading protocol used for testing the SPSLs was the one specified by the 2005 AISC seismic provisions for eccentrically braced frames (EBFs). Hysteretic behavior of both restrained and unrestrained links are shown in Figs. 13(a) and 14(a), respectively. A comparison of the results obtained accompanied by an analytical investigation is presented in the companion paper (El-Bahey and Bruneau 2011).

Specimens restrained against out-of-plane buckling using the fiber-reinforced plastic (FRP) panels almost observed the same trend of behavior during testing. For illustration, a brief description of the test performed on the SPSL presented in Fig. 13(a) is presented. At $\gamma_{tot} = 0.002$ rad, and loss of stiffness was observed in the hysteretic curves at a shear force of 150 kN. Yielding started to occur at a total rotation of 0.015 rad and a shear force of 250 kN. No buckling was observed in the wedge parts because they were designed to remain elastic (observed after removal of the FRP panels at test termination), and consequently no significant loss in strength occurred at repetitive cycles for the same rotation level. This was attributed to the fact that the middle part was the only part yielding in the specimen and was designed to yield in pure shear. At a rotation level of 0.08 rad, a drop in strength from 400 kN to 380 kN was observed; this was attributed to a fracture that might have started to propagate somehow in the middle part of the link, but this could not be confirmed or seen at that time because of the presence of the restraints. This was approximately a 20% loss in strength from the maximum strength reached, and, by definition, the specimen was deemed to have failed in performance. However, testing continued until the specimen totally fractured. Loss of strength continued at the same rotation level for every cycle performed because of the propagation of the anticipated crack. A significant loss in strength was then observed at a rotation level of 0.1 rad, and the strength dropped to almost zero. At that point, testing was terminated, and the restraints were removed to investigate the link condition at the end of the test. Fig. 13(b) shows the specimen condition after removal of the restraints.

Specimens unrestrained against out-of-plane buckling also observed similar behavior during testing. Again, a brief description of the hysteretic behavior shown in Fig. 14(a) is presented. At $\gamma_{tot} = 0.002$ rad, a loss of stiffness was observed in the hysteretic curves at a shear force of 150 kN. At a rotation level of 0.02 rad, a sudden drop in strength was observed and was attributed to the initiation of buckling that occurred in the middle part of the specimen. Up to that point, the specimen was assumed to be yielding in shear (similar to the restrained specimens); this is because of the fact that no signs of buckling were observed in the specimen from which no tension field action is assumed to develop. Because of the unavoidable geometric imperfections, buckling started to initiate in the plate, and significant strength loss was observed. The specimen then started to pick up strength gradually at each incremental cycle. Significant pinching in the hysteretic curves is also observed and expected as the plate stretches and relaxes. A strength reduction is

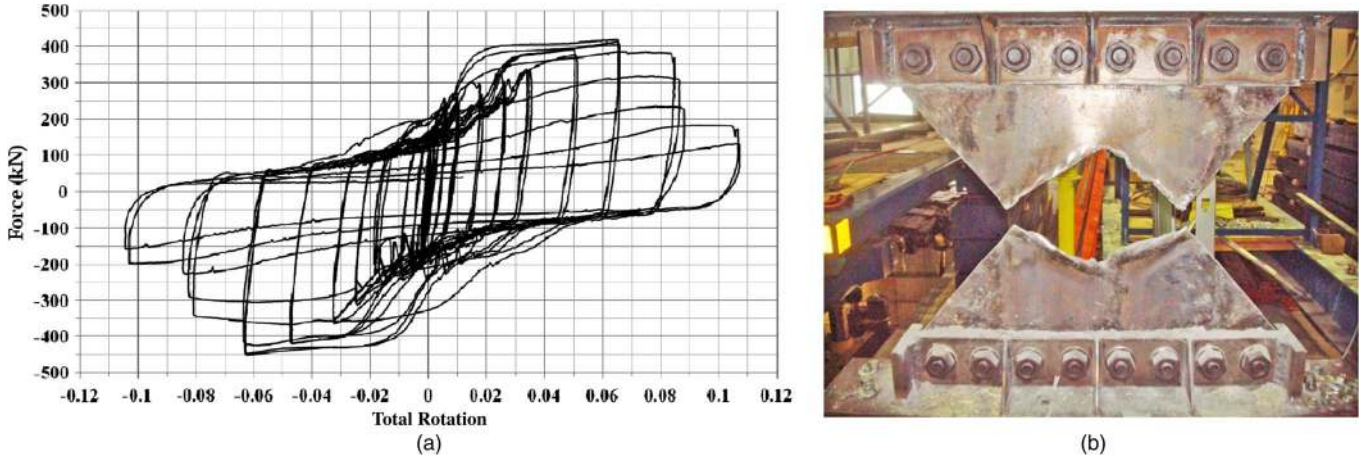

Fig. 13. (a) Link shear versus total rotation hysteretic curve for restrained specimen; (b) link condition after testing

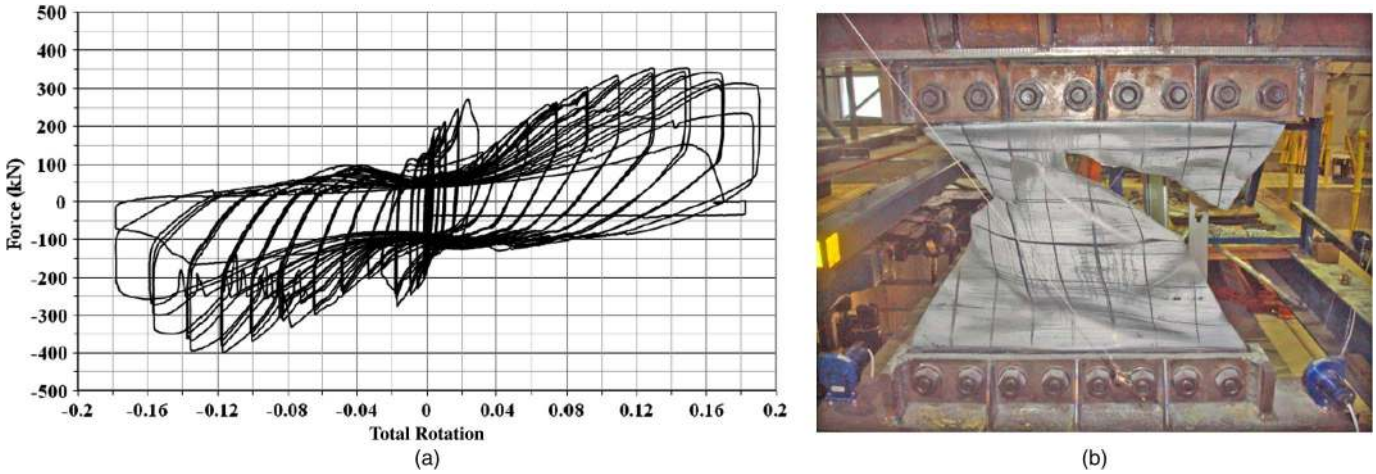

Fig. 14. (a) Link shear versus total rotation hysteretic curve for unrestrained specimen; (b) link condition after testing

also observed at each rotation level for the repetitive cycles. Progression of buckling for successive rotation levels was observed. At a rotation level of 0.13 rad, a crack at the upper-east corner of the wedge part initiated and propagated at incremental rotation levels, no significant strength loss was observed in the hysteretic curve. As the crack propagated, gradual softening in the hysteretic curve was observed in both directions. Another crack initiated in the upper-west corner at a rotation level of 0.15 rad. At that point the cracks propagated rapidly, and a significant loss in strength from 350 kN to 250 kN was observed in the negative side of the curve at a rotation level of 0.16 rad; that is approximately a 30% loss in strength. At the same rotation level at repetitive cycles, the specimen totally fractured, and the strength dropped to zero as shown in Fig. 14(b).

Conclusion

The structural fuse concept for bridges has been investigated and validated through an experimental project for a 2/3-scale proposed twin-column bridge pier bent concept using SPSLs and BRBs as a series of structural fuses. Quasi-static tests were performed to investigate the effectiveness of adding the structural fuses on the overall performance of the bent by increasing its strength and stiffness, and by providing seismic energy dissipation while keeping the bridge columns elastic. Results obtained have demonstrated the effectiveness of the proposed concept as an implementation of structural fuses in a bridge application. All specimens tested in this experimental program exhibited stable force-displacement behavior, with little pinching of hysteresis loops until the significant accumulation of damage at large drifts. Over the range of structural fuse behavior, columns remained elastic and seismic energy dissipation was limited to the structural fuses. An analytical investigation conducted to replicate the observed behavior of all specimens is presented in a companion paper (El-Bahey and Bruneau 2011).

Acknowledgments

This research was supported in part by the Federal Highway Administration under contract number DTFH61-07-C-00020 to the MCEER. The donation of the bi-steel panels by Corus Bi-Steel and the BRBs by Star Seismic is also sincerely appreciated. However, any opinions, findings, conclusions, and recommendations presented in this paper are those of the writers and do not necessarily reflect the views of the sponsors.

References

AASHTO LRFD. (2009). *Bridge design specifications, customary U.S. units, with 2008 interim revisions*, American Association of State Highway and Transportation Officials, Washington, DC.

Aiken, I., Mahin, S., and Uriz, P. (2002). "Large-scale testing of buckling restrained braced frames." *Proc. Japan Passive Control Symp.*, Tokyo Institute of Technology, Yokohama, Japan, 35–44.

Applied Technology Council (ATC). (1992). "Guidelines for seismic testing of components of steel structures." *Rep. 24*, Applied Technology Council, Redwood City, CA.

Berman, J. W., and Bruneau, M. (2005). "Approaches for the seismic retrofit of braced steel bridge piers and proof-of-concept testing of a laterally stable eccentrically braced frame." *Technical Rep. MCEER-05-0004*, Multidisciplinary Center for Earthquake Engineering Research, Buffalo, NY.

Black, C., Makris, N., and Aiken, I. (2002). *Component testing, stability analysis and characterization of buckling-restrained unbonded braces*, Pacific Earthquake Engineering Research Center, Univ. of California, Berkeley, CA.

Bowerman, H., Gough, M., and King, C. (1999). *Bi-steel design and construction guide*, British Steel, Scunthorpe, U.K.

Bruneau, M., Sarraf, M., Zahrai, S. M., and Alfawakhiri, F. (2002). "Displacement-based energy dissipation systems for steel bridges diaphragms." *J. Constr. Steel Res.*, 58(5–8), 801–817.

Clark, P., Aiken, I., Kasai, K., and Kimura, I. (2000). "Large-scale testing of steel unbonded braces for energy dissipation." *Proc. Structural Congress*, ASCE/SEI, Philadelphia.

Conner, J., Iwata, M., and Huang, Y. (1997). "Damage-controlled structures. I: Preliminary design methodology for seismically active regions." *J. Struct. Eng.*, 123(4), 423–431.

El-Bahey, S., and Bruneau, M. (2010). "Analytical development and experimental validation of a structural-fuse bridge pier concept." *Technical Rep. MCEER Rep. 10-0005*, Multidisciplinary Center for Earthquake Engineering Research, Buffalo, NY.

El-Bahey, S., and Bruneau, M. (2012). "Bridge piers with structural fuses and bi-steel columns. II: Analytical investigation." *J. Bridge Eng.*, 17(1), 36–46.

Fintel, M., and Ghosh, S. (1981). "Structural fuse: An inelastic approach to seismic design of buildings." *Civ. Eng.*, 51(1), 48–51.

Fujimoto, M., Wada, A., Saeki, E., Watanabe, A., and Hitomi, Y. (1988). "A study on the unbonded brace encased in buckling-restraining concrete and steel tube." *J. Struct. Constr. Eng., AIJ*, 34(034B), 249–258 (in Japanese).

Goodyear, D., and Sun, J. (2003). "New developments in cable-stayed bridge design, San Francisco." *Struct. Eng. Int.*, 13(1), 59–63.

Hasegawa, H., Takeuchi, T., Iwata, M., Yamada, S., and Akiyama, H. (1999). "Experimental study on dynamic behavior of unbonded-braces." *J. Architectural Build. Sci.*, 114(1448), 103–106.

Huang, Y., Wada, A., Iwata, M., and Mahin, S. (2002). "Design of damage-controlled structures." *Innovative approaches to earthquake engineering*, WIT Press, Billerica, MA, 85–118.

Iwata, M., Kato, T., and Wada, A. (2000). "Buckling-restrained braces as hysteretic dampers." *Proc., Behavior of Steel Structures in Seismic Areas STESSA 2000*, Balkema, Rotterdam, Netherlands, 33–38.

Lopez, W., Gwie, D., Saunders, M., and Lauck, T. (2002). "Lessons learned from large-scale tests of unbonded braced frame subassemblage." *Proc., 71st Annual Convention*, Structural Engineers Association of California, Sacramento, CA, 171–183.

López, W., and Sabelli, R. (2004). "Seismic design of buckling-restrained braced frames." ⟨http://www.steeltips.org/steeltips/tip_details.php?id=76⟩ (2011).

Mamoru Iwata, M. M. (2006). "Buckling-restrained brace using steel mortar planks; performance evaluation as a hysteretic damper." *Earthquake Eng. Struct. Dyn.*, 35(14), 1807–1826.

Reina, P., and Normile, D. (1997). "Fully braced for seismic survival." *Eng. News-Rec.*, 34–36.

Roeder, C., and Popov, E. (1977). "Inelastic behavior of eccentric braced steel frames under cyclic loadings." *Rep. No. UCB-77/17*, Earthquake Engineering Research Center, Univ. of California, Berkeley, CA.

Sabelli, R., Mahin, S., and Chang, C. (2003). "Seismic demands on steel braced frame buildings with buckling-restrained braces." *Eng. Struct.*, 25(5), 655–666.

Saeki, E., Maeda, Y., Nakamura, H., Midorikawa, M., and Wada, A. (1995). "Experimental study on practical-scale unbonded braces." *J. Struct. Constr. Eng., AIJ*, 476, 111–120 (in Japanese).

Shimizu, K., Hashimoto, J., Kawai, H., and Wada, A. (1998). "Application of damage control structure using energy absorption panel." *Structural Engineering World Wide*, *Paper No. T105-2*, Elsevier Science, Amsterdam, Netherlands.

Vargas, R., and Bruneau, M. (2009a). "Analytical response and design of buildings with metallic structural fuses. I." *J. Struct. Eng.*, 135(4), 386–393.

Vargas, R., and Bruneau, M. (2009b). "Experimental response of buildings designed with metallic structural fuses. II." *J. Struct. Eng.*, 135(4), 394–403.

Wada, A., Connor, J. J., Kawai, H., Iwata, M., and Watanabe, A. (1992). "Damage tolerant structures." *Proc., Fifth U.S.–Japan Workshop on the Improvement of Structural Design and Construction Practices, ATC-15-4*, Applied Council Technology, Redwood City, CA, 27–39.

Wada, A., and Huang, Y. (1995). "Preliminary seismic design of damage tolerant tall building structures." *Proc., Symp. on a New Direction in Seismic Design*, Architectural Institute of Japan, Tokyo, 77–93.

Wada, A., and Huang, Y. (1999). "Damage-controlled structures in Japan." *Proc., U.S-Japan Workshop on Performance-Based Earthquake Engineering Methodology for Reinforced Concrete Building Structures*, Vol. 10, Pacific Earthquake Engineering Research Center, Univ. of California, Berkeley, CA, 279–289.

Wada, A., Huang, Y., and Iwata, M. (2000). "Passive damping technology for buildings in Japan." *Prog. Struct. Eng. Mater.*, 2(3), 335–350.